AD-A184 070 DEFORMATION MECHANISMS OF THERMOSTRUCTURAL MATERIALS (U) CRYSTAL GROWTH AND MATERIALS TESTING ASSOCIATES LANHAM MD R J ARSENAULT ET AL. 20 JUL 87 162 1/1

UNCLASSIFIED N00014-85-C-2240 F/G 11/6.1 NL

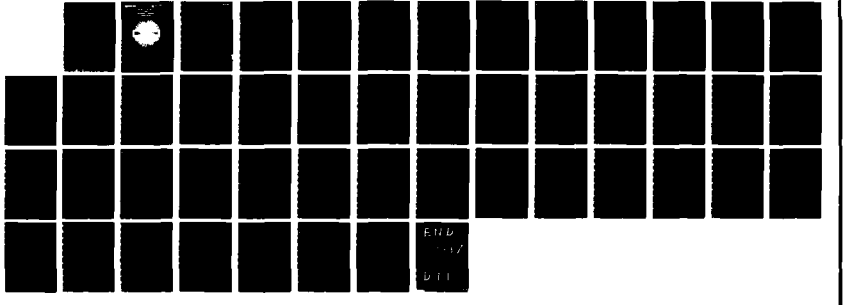

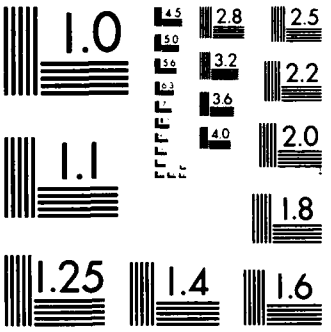

MICROCOPY RESOLUTION TEST CHART
NATIONAL BUREAU OF STANDARDS-1963-A

(12)

CRYSTAL GROWTH AND MATERIALS TESTING ASSOCIATES

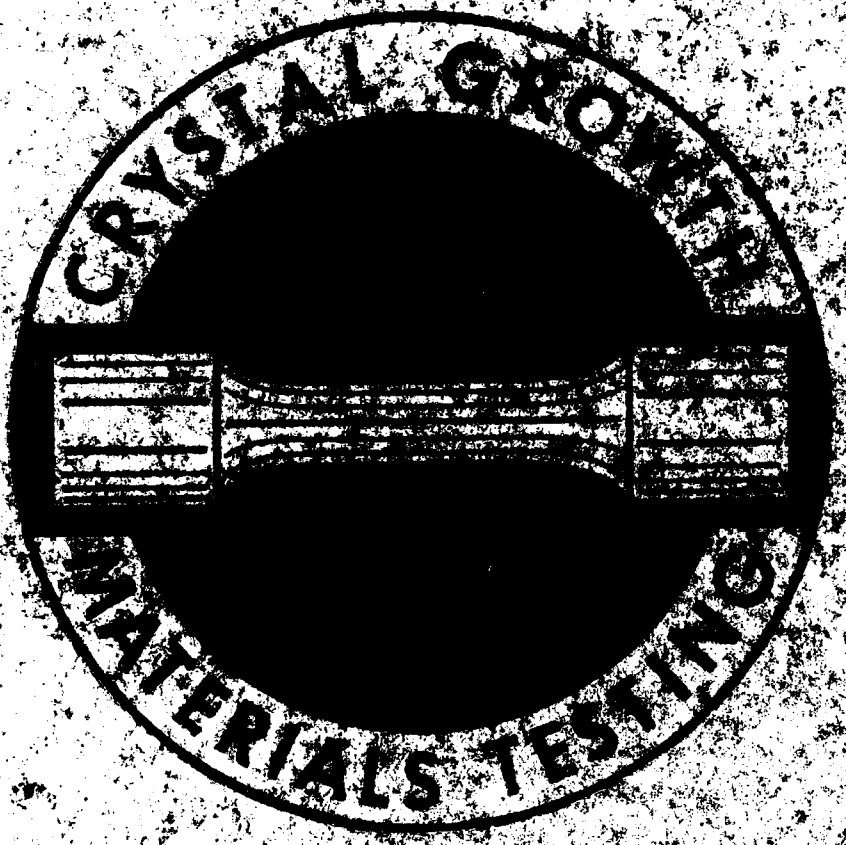

R. J. Arsenault
Director
6918 Lamont Drive
Lanham, Maryland 20706

Phone Number
(301) 454-4075

AD-A182936

REPORT DOCUMENTATION PAGE

1a. REPORT SECURITY CLASSIFICATION	1b. RESTRICTIVE MARKINGS
2a. SECURITY CLASSIFICATION AUTHORITY	3. DISTRIBUTION/AVAILABILITY OF REPORT Approved for public release Distribution unlimited
2b. DECLASSIFICATION/DOWNGRADING SCHEDULE	
4. PERFORMING ORGANIZATION REPORT NUMBER(S) 162	5. MONITORING ORGANIZATION REPORT NUMBER(S)
6a. NAME OF PERFORMING ORGANIZATION Crystal Growth and Materials Testing Associates 6b. OFFICE SYMBOL (If applicable)	7a. NAME OF MONITORING ORGANIZATION
6c. ADDRESS (City, State and ZIP Code) 6918 Lamont Drive Lanham, MD 20706	7b. ADDRESS (City, State and ZIP Code)
8a. NAME OF FUNDING/SPONSORING ORGANIZATION Naval Research Lab 8b. OFFICE SYMBOL (If applicable)	9. PROCUREMENT INSTRUMENT IDENTIFICATION NUMBER N00014-85-C-2240
8c. ADDRESS (City, State and ZIP Code) Disbursing Office ATTN: Code 1332 Naval Research Lab, Washington, DC 20375-5000	10. SOURCE OF FUNDING NOS. PROGRAM ELEMENT NO. / PROJECT NO. / TASK NO. / WORK UNIT NO
11. TITLE (Include Security Classification) Deformation Mechanisms of Thermostructural Materials	
12. PERSONAL AUTHOR(S) R.J. Arsenault, N. Louat, P. Shahinian, A.K. Singh, T. Chaki	
13a. TYPE OF REPORT FINAL 13b. TIME COVERED FROM 5-20-85 TO 5-20-87	14. DATE OF REPORT (Yr., Mo., Day) 20 July 1987 15. PAGE COUNT 44
16. SUPPLEMENTARY NOTATION N/A	
17. COSATI CODES FIELD / GROUP / SUB. GR.	18. SUBJECT TERMS (Continue on reverse if necessary and identify by block number) Cobalt, [illegible]

19. ABSTRACT (Continue on reverse if necessary and identify by block number)

In this final report are discussed the results obtained in a two year investigation by Crystal Growth and Materials Testing Associates of the deformation mechanisms of thermostructural materials. This report is divided into three portions: 1. Some effects of the presence of particles near free surfaces; 2. Improvement of turbine blades and other components by hot isostatic pressing; 3. Thermal and thermo-mechanical fatigue of superalloy Rene 80 coated with CoCrAlY.

20. DISTRIBUTION/AVAILABILITY OF ABSTRACT UNCLASSIFIED/UNLIMITED ☐ SAME AS RPT. ☐ DTIC USERS ☐	21. ABSTRACT SECURITY CLASSIFICATION
22a. NAME OF RESPONSIBLE INDIVIDUAL Richard J. Arsenault, Ph.D.	22b. TELEPHONE NUMBER (Include Area Code) (301) 454-4075 22c. OFFICE SYMBOL

DD FORM 1473, 83 APR EDITION OF 1 JAN 73 IS OBSOLETE

Report No. 162

DEFORMATION MECHANISMS OF THERMOSTRUCTURAL MATERIALS

Prepared by:

Crystal Growth and Materials Testing Associates

Dr. R.J. Arsenault, Director

Dr. T. Chaki

Dr. N. Louat

Dr. P. Shahinian

Dr. A.K. Singh

20 July 1987

Final Report for Contract No. N00014-85-C-2240

Prepared for:

Disbursing Office
ATTN: Code 1332
NAVAL RESEARCH LABORATORY
Washington, DC 20375-5000

TABLE OF CONTENTS

FINAL REPORT

DEFORMATION MECHANISMS OF THERMOSTRUCTURAL MATERIALS

I. INTRODUCTION

In this final report are discussed the results obtained in a two year investigation by Crystal Growth and Materials Testing Associates of the deformation mechanisms of thermostructural materials. This report is divided into three portions: 1. Some effects of the presence of particles near free surfaces; 2. Improvement of turbine blades and other components by hot isostatic pressing; 3. Thermal and thermo-mechanical fatigue of superalloy Rene' 80 coated with CoCrAlY.

The following is a brief outline of each of these topics.

Diffusion of oxygen through columnar grain boundaries formed during processing of coatings can lead to internal oxidation and the formation of oxide inclusions in close proximity to a free surface. Since oxidation is accompanied by an increase in volume, large misfit strains are generated at the inclusions. In view of the close proximity of a free surface, the misfit induces large hydrostatic stresses in the elastic medium surrounding the inclusion. These stresses have been determined exactly for a cylindrical inclusion using linear elasticity theory, and using these exact solutions, stresses have been estimated for a spherical inclusion. These stresses seem to be significant in that they could lead to fracture or prismatic dislocation punching in a coating. In addition, it is shown that these hydrostatic stresses can accelerate kinetics of diffusion of the damaging species and lead to rapid deterioration of the coating. Furthermore, the stress can induce the

formation of pits at the coating surface which can grow into cracks and lead to failure of the coating.

The objective of the HIP (hot isostatic pressing) investigation was to develop optimum conditions for the improvement of cast IN 100 (PWA 658) blades. There have been several efforts in the past in various laboratories to develop proper HIP conditions that can not only close the casting porosity but also refine the microstructure. The results of these investigations pertaining to the influence of HIP on creep properties of IN 100 have varied.

In the present program thermal and thermo-mechanical fatigue of superalloy Rene' 80 was studied. The effect of post heat treated electron beam physical vapor deposition (EBPVD) CoCrAlYcoating was investigated To get the base line data, creep tests at elevated temperatures were performed for the coated and uncoated specimens. To understand the effect of the coating, detailed characterization of the microstructure at the interface between the coating and the substrate was done.

II. SOME EFFECTS OF THE PRESENCE OF PARTICLES NEAR FREE SURFACES

ABSTRACT

Diffusion of oxygen through columnar grain boundaries formed during processing of coatings can lead to internal oxidation and the formation of oxide inclusions in close proximity to a free surface. Since oxidation is accompanied by an increase in volume, large misfit strains are generated at the inclusions. In view of the close proximity of a free surface, the misfit induces large hydrostatic stresses in the elastic medium surrounding the inclusion. These stresses have been determined exactly for a cylindrical inclusion using linear elasticity theory and using these exact solutions, stresses have been estimated for a spherical inclusion. These stresses seem to be significant in that they could lead to fracture or prismatic dislocation punching in a coating. In addition, it is shown that these hydrostatic stresses can accelerate kinetics of diffusion of the damaging species and lead to rapid deterioration of the coating. Furthermore, the stress can induce the formation of pits at the coating surface which can grow into cracks and lead to failure of the coating.

INTRODUCTION

Protective coatings are used for almost all of the superalloy turbine blades to reduce the kinetics of damage due to high temperature oxidation or corrosion. In addition to protection against oxidation or corrosion, coatings are also used to provide thermal barriers to reduce the substrate temperature. The protective properties of most of the coatings used today, such as

aluminides or MCrAlY, are due to the formation of a thin oxide scale on the surface of the coating. The degree of adherence of the oxide scale to the coating and the rapidity with which the scale replenishes itself are important factors in determining the life of the coating. It has been observed that addition of reactive elements such as Y, H, etc., tends to improve the oxidation protection. Several mechanisms have been proposed to account for this improvement. The most important factor in all of these is the fact that these elements oxidize rapidly to form their respective oxides.

In many cases the damaging species such as oxygen or sulphur can diffuse through grain boundaries and internally oxidize the reactive elements. This is more predominant for coatings that have remanent columnar grains formed during processing. Such an internal oxidation of elements such as Y, Hf, Ni, Cr, etc., can cause formation of oxide inclusions in close proximity to the free surface. Since oxide formation results in increase in volume, such an inclusion near a free surface can induce very high hydrostatic stresses in the surrounding elastic medium. The object of this paper is to estimate analytically the magnitude of these stresses and their effects on subsequent degradation of the coating. For example, these stresses are condusive to the formation of pits and also enhance the rate of diffusion which is involved in these processes. Pit formation is a precursor of cracking and fracture.

Diffusion in solids, with the possible exception of that involving interstitial atoms, requires the presence and motion of vacancies. In fact, the diffusion coefficient, D, can be expressed as

$$D = CF$$

where C is the concentration of vacancies and F is a frequency factor. In general, F and C are functions of temperature while C, in particular, varies with stress. Thus, for a system at equilibrium the local concentration of vacancies at temperature T is:

$$C = C_o e^{\Delta\Omega/kT},$$

where Ω is the formation volume of a vacancy and Δ the local dilatational stress; k is, as is usual, Boltzmann's constant. We now note, that if Δ were to reach values corresponding to a few (n) percent elastic strain, we find with T = 900°C that $\Delta\Omega/kT \sim 1.6n$. This would correspond to an increase in D by a factor of ~ 100 when n = 3.

Because these numbers indicate the possibility of significant increases in the rates of diffusion consequent on the existence of large values of Δ and because it appears a priori that such values could arise in the neighborhood of oxide particles formed in the proximity of free surfaces, we have here made a formal calculation of such stresses.

To begin, we note that to first order in linear elasticity the total dilation introduced in an infinite solid by the presence of a misfitting inclusion is zero. Furthermore, when the inclusion is spherical and the stresses around it have spherical symmetry the dilation is zero everywhere, that is to say, the sum of the three principal stresses is zero at every point. This behavior breaks down at a free surface since the stress normal to that surface must vanish. That is to say the surface must distort so as to produce a stress which just balances it.

ANALYSIS

For elastic equilibrium shear stresses in and direct stresses normal to a free surface must vanish. Thus, in the case of a sphere of radius a, centered a distance h below a planar surface of an elastically isotropic solid and under a uniform, say compressive, pressure ρ (Fig. 1) the stresses [1] at the surface, at a radial distance r are:

$$\sigma_N = - p\, a^3 \frac{(2h^2 - r2)}{(r^2 + h^2)^{5/2}};$$

$$\sigma_s = \frac{3}{2} p\, a^3 \frac{rh}{(r^2 + h^2)^{5/2}}.$$

The stresses due to the sphere are to be just balanced by those developed by surface displacements. Of these, the shear stresses σ_s are annulled by supposing another identical spherical particle to exist at the image point of the first.

We then have:

$$\sigma_N = -2pa^3 \frac{(2h^2 - r^2)}{(r^2 + h^2)^{5/2}}; \qquad \sigma_s = 0. \tag{1}$$

The problem has then become one of finding the normal surface displacements which give surface stresses which are equal and opposite to those of (1) and subsequently to use these same displacements to determine the dilatational stresses at arbitrary points.

This end can be achieved in a number of ways including the Hankel transform method developed by Sneddon [2] but we shall follow that developed by

Leibfried [3] and Louat [4]. There, one represents the displacements as the aggregate of infinitesimal circular dislocation rings and expresses the condition of equilibrium in the form:

$$\frac{\mu\lambda}{2\pi(1-\nu)} \int_0^\infty f(R)\ R\ dR \int_0^{2\pi} \frac{(R-r\cos\alpha)\, d\alpha}{(R^2 + r^2 - 2rR\cos\alpha)^{5/2}}\ \sigma(r) = 0, \qquad (2)$$

where R and α are used as integration variables. Here, μ is the shear modulus and the ν the Poisson's ratio of the material. λ is the unit of displacement which at radius R is U(R). The function f(R) is the dislocation distribution density and is the derivative of U(R). Thus,

$$f(R) = \frac{dU}{dR}$$

After some manipulation it is found that

$$f(r) = \frac{-1}{\pi^2 A} \frac{d}{dr} \int_r^\infty \frac{\zeta\, d\zeta}{(\zeta^2 - r^2)^{\frac{1}{2}}} \frac{d}{d\zeta} \int_0^\zeta \frac{dR}{(\zeta^2 - R^2)^{\frac{1}{2}}} \left\{ \int \sigma(R)\, dR + \frac{b}{R} \right\}$$

where b is a constant of integration. Substitution here for $\sigma(R)$ from (1) gives:

$$f(r) = \frac{ba^3hr}{\pi A(r^2 + h^2)^{5/2}}, \qquad a = \frac{\mu\lambda}{2\pi(1-\nu)} \cdot \qquad (3)$$

Now the stresses due to loop of dislocation of Burger's vector b and radius r are known and in principle those to an array of such loops follows from integration. Here, however, the integrals appear to be analytically

intractable in the general case. We content ourselves therefore with the special case of stresses at points which lie on the normal to the free surface which passes through the center of the sphere, along the y axis in Fig. 1.

In this case the dilatational stress at a distance y from the plane of the loop is:

$$\frac{1+\nu}{3(1-\nu)} \quad \mu b \quad \frac{r^2}{(r^2+y^2)^{3/2}}$$

and the total stress due to all loops is, on substituting from (3),

$$(1+\nu)\, pa^3 h \int_0^\infty \frac{r^3}{(r^2+h^2)^{5/2}} \frac{dr}{(r^2+y^2)^{3/2}} = \frac{2}{3}(1+\nu)\frac{pa^3}{(h+y)^3} \equiv \Delta_s. \tag{4}$$

An examination of (4) shows, as seems reasonable, that Δ_s is maximum when the sphere just touches the surface.

The failure of the analysis to provide values for Δ at off-axis positions can be rectified in part by resorting to numerical integration. The resultant tables of numbers, while an end in themselves would, however, be of little help in further analysis. Accordingly, we compare this result with that obtained from the consideration of an infinite circular cylinder under the same pressure and centered at the distance h from a planar free surface. This is a two-dimensional problem and closed-form solutions can be obtained even at off-axis positions. Comparison of the two solutions provide us a scaling factor using which the results for a spherical inclusion can be estimated.

Here, we can employ the approach introduced by Louat [5] which is the two-dimensional analogue of the procedure employed above. In place of (2) the equation of equilibrium becomes

$$A \int_{-\infty}^{\infty} \frac{f(t)}{t - x}\, dt + 2\sigma_n(x) = 0 \qquad (5)$$

where $\sigma_n(x)$ is the normal stress at the position of the free surface:

$$-pa^2 \left[\frac{(x^2 - h^2)}{(x^2 + h^2)}\right]^2 ,$$

developed by a circular cylinder of radius a centered a distance h from the free surface when it is under an internal compressive pressure p.

The inversion of (5) is straightforward, yielding:

$$f(x) = \left[\frac{2pa^2hx}{3\pi A(h^2 + x^2)}\right]^2 .$$

Then, for rectangular coordinates centered so that the cylinder axis is located at 0, h, the dilatational stress at the point x,y is

$$4pa^2(1 + \nu)\, h \int_{-\infty}^{\infty} \left[\frac{t}{(h^2 + t^2)}\right]^2 \left[\frac{t - x}{(t - x)^2 + y^2}\right]^2 dt$$

$$= \frac{2p(1 + \nu)ha^2}{3} \left[\frac{(h + y)^2 - x^2}{\left[(h + y)^2 + x^2\right]}\right]^2 \equiv \Delta_c$$

Returning to a consideration of the spherical particle it may in view of (3) be anticipated that for $x >> h$

$$\Delta_s \simeq \frac{2}{3}\ (1 + \nu)\ p\ \frac{a^3}{x^3}\ .$$

Then since $x << h$, Δ_s is of the same form as Δ_c, it is to be expected that the extrapolated form;

$$\Delta_s = \frac{2}{3}\ (1 + \nu)\ pa^3\ \frac{r^2 - (h + y)^2}{\left[r^2 + (h + y)^2\right]^{5/2}} \qquad (6)$$

should provide a reasonable approximation almost everywhere.

It remains to relate the internal pressure p in the particle to the misfit between it and the lattice. This is readily achieved using Love's [6] expression for the bulk modulus of the material around a hole:

$$\frac{4}{3}\ \mu_m$$

where μ_m is its shear modulus.

We suppose the hole initially too small (or large) for the particled but that it fits after application of a hydrostatic pressure:

$$K_p\ \Delta_o$$

where K_p is the bulk modulus of the particle and Δ_o the necessary dilatation. In a thought experiment the particle is inserted in the hole and the pressure constraint released. Equilibrium results when the pressure in the particle equals that just outside it and so when

$$p = K_p (\Delta_o - \Delta_f) = \frac{4}{3} \mu_m \Delta_f$$

where Δ_f, the dilatation,

$$= \frac{3K_p \Delta_o}{4\mu_m + 3K_p}$$

so that

$$p = \frac{4 K_p \mu_m}{4\mu_m + 2K_p} \Delta_o \tag{7}$$

When particle and matrix have the same value of Poisson's ration ($\nu = 1/3$ but different shear moduli we have from (7):

$$p = \frac{8}{3} \frac{\mu_p \mu_m}{\mu_m + 2\mu_o} \Delta_o. \tag{8}$$

For increasing values of the ratio μ_p/μ_m we have

$$\frac{8}{3} \mu_p \Delta_o < p < \frac{4}{3} \mu_m \Delta_o.$$

It would seem for the case of Ni and NiO that $\mu_p/\mu_m \sim \frac{1}{2}$. Substitution of these values in (7) gives:

$$p = \frac{2}{3} \mu_m \Delta_o$$

Here, Δ_o is given by

$$T - 1$$

where T represents the Pilling-Bedworth ratio:

$$\frac{\text{Molecular Volume of Oxide}}{\text{Atomic Volume of Metal}} .$$

In the case of Ni, T = 1.52 so that

$$\Delta_o = .52.$$

The use of this number in (9) gives unrealistically large stresses. Such stresses should be obviated through the intervention of localized fracture or through the formation of prismatic dislocation loops.

In reasonably ductile materials such as nickel-based alloys we anticipate that prismatic loops should form when the shear stresses in regions adjoining the particle are a few, say 4, percent of the elastic modulus [7]. As is readily shown these stresses are comparable to p. Accordingly, we shall suppose that $p \sim .04\ \mu m$.

Effect on Rate of Diffusion

As indicated earlier we suppose that diffusion proceeds through the agency of lattice vacancies and that the local diffusion coefficient is proportional to their local equilibrium concentration. Accordingly, for a complete description we require a solution of the diffusion equation:

$$\frac{d}{dr} D \frac{dc}{dr} + \frac{1}{r} \frac{dDc}{dr} + \frac{d}{dy} D \frac{dc}{dy} = 0;$$

$$D = D_o \exp(\Delta_o \Omega / kT) \equiv D_o \exp W(y)/kT;$$

$$W(y = 0) \equiv W(o)$$

with: $C = C_1,\ y = 0;\ C = C_2,\ (y - h)^2 + r^2 = a^2.$

Solutions for this equation do not seem to be available. Accordingly, we resort to approximation. We note that when W/kT is significant at y = 0, D varies rapidly with y and r and can be expected to deviate from D_o only in the small volume lying between the particle and the free surface. Therefore, we ignore the sphericity of the particle and consider one-dimensional diffusion along the length of a cylinder of radius ~ a. At equilibrium the diffusion flux is constant and given by:

$$J \simeq - \pi a^2 \frac{d}{dy} D(y)\ C.$$

Solving this equation we find

$$J \sim \pi a^2 \left(\frac{C_1 D_o \exp [W(o)]/kT - C_2 D_o \exp [W(h-a)]/kT}{h} \right)$$

$$\sim \frac{\pi a^3 C_1 D_o \exp \left[w(o)/kT \right]}{h} .$$

This is to be compared with that which flows when D = constant, namely:

$$J_c = 2a D_c (C_1 - C_2).$$

Thus, the ratio of these fluxes is simply

$$\exp \left[w(o)/kT \right].$$

We conclude, therefore, that diffusion of solute to a particle and hence the rate of oxidation can be increased by the presence of hydrostatic stresses developed as a consequence of that oxidation if these stresses are such that $W(o)/kT > 1$. In fact, with $p = \mu/25$ as suggested earlier we find this factor to be ~ 2.0 when T ~ 1000°C.

Surface Pitting

A second particular result of the presence of such stresses is to be noted. The Gibbs free energy G of a system is reduced, converting an initially flat free surface to a crater, Fig. 4. The extent to which this process continues may be determined from a consideration of the rate of change of G:

$$\delta G = \delta(\gamma s) - \delta \left(\int_o^v p d\nu \right)$$

Here γ is the surface energy/unit area, S is the surface area of the crater surface and v its volume. To effect such a calculation we suppose for simplicity that the crater surface is spherical in shape with radius R_m and represent its area as:

$$S = 2\pi R_m^2 (1 - \cos \theta_m)$$

where θ_m is the semi-angle subtended by the spherical cap at the center of the sphere. We suppose $R_m \sin \theta_m = h$. Again, since we are interested in the rate of change of energy and since h continually decreases as the crater deepens we shall take:

$$p = \frac{(h - s)^2 - r^2}{\left[(h - s)^2 + r^2\right]^{5/2}} \quad \frac{2p}{3} \; a^3(1 - \nu)$$

where s is the depth of the crater. We then write

$$\delta\nu = 2\pi r \, R \, d\theta \cos \theta \, (\sec \theta_m - \sec \theta) \, dR$$

and get:

$$\int_0^v p d\nu = 2\pi \int_0^R \frac{R^2}{\cos \theta_m} dR \int_0^{\sin^{-1}\frac{h}{R}} \sin \theta \, (\cos \theta - \cos \theta_m).$$

$$\frac{[h - R(1 - \cos \theta)]^2 - R^2 \sin^2\theta}{\left[[h - R(1 - \cos \theta)]^2 + R^2 \sin^2\theta\right]^{5/2}} \quad d\theta$$

$$; \quad \theta_m = \sin^{-1} \frac{h}{R}.$$

Analytical integration of this in simple form does not seem possible and we restrict ourselves to the consideration of the important case where θ_m is always small. That is, to circumstances where the crater is first forming. There we take the stress as constant and equal to $p \frac{a^3}{h^3}$ throughout the volume displaced. The energy decrement is then:

$$\frac{2}{3}(1+\nu) p \frac{a^3}{h^3} \cdot \pi R^3 \left\{ \frac{2}{3} - \cos\theta + \frac{\cos^3\theta}{3} \right\}$$

$$= \frac{2\pi}{3}(1+\nu)\, p \frac{a^3}{h^3} \cdot \frac{11}{12} R^3\theta^4 = \frac{11\pi}{18}(1+\nu)\, p\frac{a^3}{h^3} \cdot h^3\theta$$

$$= \frac{11\pi}{18}(1+\nu)\, p \frac{a^3}{h^3} \cdot h^2 s; \quad s = h\theta; \quad \theta = \sin^{-1}\frac{h}{R}.$$

Again, the surface energy is incremented by an amount:

$$2\pi R^2 (1 - \cos\theta) - \pi h^2 = \frac{\pi h^2\theta^2}{3} = \frac{\pi s^2}{3}.$$

Thus,

$$G = -\frac{11}{18}\pi(1+\nu)\, p \frac{a^3}{h^3}\, h^2 s + \frac{\pi s^2 \gamma}{3}$$

where γ is the specific surface energy. We then have

$$\frac{dG}{dS} = -\frac{11}{6}\,\pi(1+\nu)\,p\,\frac{a^3}{h^3}\,h^3 + \frac{2\pi}{3}\,S\,\gamma \qquad (10)$$

Clearly, this is always negative for S sufficiently small. Therefore, a crater will commence to form for all stresses p. According to (10), it reaches equilibrium when

$$S \simeq \frac{2}{3}\,(1+\nu)\,\frac{pa^3}{\gamma h}$$

Thence, taking $s \sim a \sim h/2$, we find

$$p \sim \gamma/a$$

This, for $h \sim 1\mu$, is technically a very small stress.

We conclude that the presence of expanding particles close to a free surface will lead to the formation of craters in that surface.

CONCLUSIONS

We have calculated the hydrostatic stresses developed when the stresses due to a misfitting particle interfere with a planar free surface. These hydrostatic stresses can be important in accelerating oxidation and corrosion through increased vacancy concentration and as a direct consequence, increased rates of diffusion. Additionally, their presence can lead to the formation of pits.

ACKNOWLEDGEMENTS

The authors express their appreciation to Dr. V. Provenzano for many stimulating discussions.

REFERENCES

1. S. Timoshenko and J.N. Goodier, *Theory of Electricity*, McGraw-Hill, New York, 2nd Ed. (1951) 359.

2. I.N. Sneddon, *Fourier Transforms*, McGraw-Hill (1951) 470-490.

3. G. Liebfried and Z. Angew, *Phys.* **6** (1954) 251.

4. N. Louat, *Int. J. Eng. Sci.* **10** (1972) 665.

5. N. Louat, *Nature* **196** (1962) 1081.

6. A.E.H. Love, *A Treatise on the Mathematical Theory of Electricity*, University Press, Cambridge (1920).

7. G.E. Weatherly, *Phil. Mag.* **17** (1968) 791.

III. IMPROVEMENT OF TURBINE BLADES AND OTHER COMPONENTS BY HOT ISOSTATIC PRESSING

INTRODUCTION

The objective of this investigation is to develop optimum HIP (hot isostatic pressing) conditions for the improvement of cast IN 100 (PWA 655) blades. There have been several efforts[1-4] in the past in various laboratories to develop proper HIP conditions that can not only close the casting porosity but also refine the microstructure. The results of these investigations pertaining to the influence of HIP on creep properties of IN 100 have varied. A detailed review of these studies was presented in Ref. 5.

Our previous studies[6] on IN 713 (PWA 655) led us to believe that improvement in creep rupture properties can only be accomplished by the judicious selection of HIP conditions such that refinement in microstructure occurs during HIP. Control of the size and distribution of γ' precipitates is a key factor in insuring the improvement in creep properties. Careful and systematic analysis of microstructure and chemistry of IN 100 cast specimens revealed that a significant amount of eutectic γ' is formed during the casting process. This has an important bearing in terms of the HIP temperature since complete dissolution of the eutectic γ' does not occur unless the temperature is close to the eutectic melting point. On the other hand, such a high temperature can lead to microstructural instabilities including carbide dissolution and grain growth which can contribute to deterioration of properties. Another factor that also has bearing in terms of evaluation of the HIP processes is the γ' precipitate size and distribution in the as-cast specimens. If the starting γ' size in the as-cast specimens is extremely

fine, as is the case in our creep rupture specimens, the rupture life of the base line material is relatively high and the observed improvement in life as a result of HIP may not be significant, whereas, the analysis of the microstructure of the new IN 100 blades that were obtained from NARF-Norfolk showed significantly coarser γ' structure than was observed in the vender provided cast-creep rupture specimens. In view of the these observations, we note that the improvement in properties that were observed in the present study are more conservative because of the fact that the starting microstructure is extremely fine. Noticeably greater improvement in life, however, is anticipated for blade specimens that have initially coarser microstructure in the as-cast condition.

MICROSTRUCTURE

Microstructural studies of non-HIP (H-A, H-B and H-C) specimens were done using optical, scanning and transmission electron microscopy. In the scanning electron micrographs , significant casting porosity can be noted in the non-HIP specimen. In addition, the microstructure shows four major phases, namely: γ, γ', and eutectic γ-γ' and several carbides. None of the HIP specimens H-A, H-B and H-C contains any porosity. Therefore, all of the HIP conditions used are effective in closing the casting porosity. Significant microstructural changes, however, were found to occur as a result of HIP. For example, γ' coarsening was observed for all the HIP conditions. Primary carbides remained unaltered. The amount of the eutectic γ-γ' decreases with increase in the HIP temperature. Very small amounts of the eutectic γ-γ' were found in H-B and H-C specimens. Large volume frac-

tions of the γ' phase were noted in all of the specimens.

CREEP RUPTURE

Creep rupture experiments were carried out at 1800°F and 29 ksi. To determine the effectiveness of HIP on life, a histogram was plotted. The spread in creep rupture life was less for the HIP specimens. Absence of casting porosity contributed to the reduced scatter in the results. In addition, creep rupture life depends on the HIP temperature. HIP specimens at H-A have the maximum creep rupture life. The rupture lives of specimens HIP processed at H-B and H-C are nearly the same but much lower than that at H-A. The lower life at higher temperatures is probably due to increased oxidation of the specimens. There are also some noticeable changes in grain boundary chemistry during the higher temperature HIP (H-B and H-C). Such changes are anticipated due to increased dissolution of γ-γ' eutectic during HIP.

Microstructural changes in ruptured specimens are the same for both the non-HIP and the HIP conditions. The cuboidal γ' changes into platelet form in the presence of stress. There is no change in the γ' in the threaded section since the applied stress was small. Comparison of the microstructure structure at the gauge and threaded sections reveals the coarsening of γ' under creep.

DISLOCATION SUBSTRUCTURE

A transmission electron microscopic study was performed on the non-HIP and the HIP (H-A) specimens. Most of the γ' are of cuboidal shape and their

interfaces with γ are free of dislocations. However, occasionally the presence of some interfacial and matrix dislocations could be seen in some regions. These dislocations are of $\frac{1}{2}$ [110] type. The shape of γ' precipitates that have dislocations at the interfaces are irregular. The microstructures of the HIP (H-A) specimens show significant coarsening of γ'. Many γ' precipitate particles in this case are of irregular shape and many have dislocations at the interfaces. Some of the γ' are still cuboidal and free of any interfacial dislocations. No significant difference is noted between ruptured non-HIP and the HIP specimens. Lamaller growth of γ' is a very dominant feature for the sections parallel to the stress axis. There are interfacial dislocation networks around the γ' precipitates. Such network formations were observed in all the non-HIP and the HIP specimens. Morphological changes of γ' observed after creep are the same in all specimens, irrespective of conditions used. On the other hand, deformation mechanisms do vary with the applied stress and test temperature. One of the non-HIP specimens was tested at 94 ksi/1400°F and the microstructure at a gauge section indicates the cutting of γ' by dislocations. The micrograph shows the cuboidal γ' and slip traces crossing through the γ'. This is in contrast to the deformation mechanism operating at high temperature where dislocations bypass the particles leaving Orowan loops which subsequently form a interfacial dislocation network. Additional creep experiments and the microstructural studies at 94 ksi/1400° are presently underway.

CONCLUSION

Optimum HIP conditions for the improvement of creep rupture life for IN 100 have been established. These correspond to H-A . Experiments are presently underway to evaluate the effect of this optimum HIP on the creep rupture properties at 1400°F and 94 ksi.

REFERENCES

1. D.C. Stewart, Presentation at Naval Air Systems Command, Pratt & Whitney Aircraft DPD, Sept. 21, 1983.

2. P. Shahinian and K. Sadananda, *Application of Hot Isostatic Pressing to Improve Cast Turbine Blade Alloy Life*, NRL Memorandum Report 5192, Naval Research Laboratory, Sept. 30, 1983.

3. Anon, Howmet Data, 1977.

4. D.C. Stewart and G.T. Bennet, *HIP Rejuvenation of Damaged Blades*, AFWAL TR-80-4043, Air Force Materials Laboratory, Wright-Patterson AFB, OH, May 1980.

5. P. Shahinian and K. Sadananda, *Hot Isostatic Pressing of Gas Turbine Cast Superalloys*, NRL Memorandum Report 5817, Naval Research Laboratory, August 29, 1986.

6. K. Sadananda, A.K. Singh and P. Shahinian, *Improvement in Life of Cast Turbine Blade Alloy by Hot Isostatic Pressing*, NRL Memorandum Report 5618, Naval Research Laboratory, August 14, 1985.

TABLE I

Chemical Composition of Alloy IN 100 (PWA 658)

Element	PWA 658 (IN 100)
C	0.169 wt%
Mn	0.009
P	0.005
S	0.003
Si	0.037
Ni	Bal
Cr	9.36
Mo	3.09
Co	14.32
Fe	0.140
V	0.76
Ti	4.83
Al	5.75
Zr	0.035
B	0.0112
Pb	0.00001
Bi	0.00002
Se	0.00003
Te	0.00001
Ti	0.00003

IV. THERMAL AND THERMO-MECHANICAL FATIGUE OF SUPERALLOY RENÉ 80 COATED WITH CoCrAlY ALLOY

A. INTRODUCTION

Nickel-base superalloy René 80 (René 80 is the trademark owned by General Electric Company) is used as a high temperature blade material[1] in turbine engines. Its excellent strength[2,3] and creep [1,2,4,5,6] properties at high temperature are noteworthy. But corrosion[7] due to the environment at high temperature reduces its life. Hot corrosion attack may occur at temperatures in the range 600-1000°C operating in combusion or marine environments. The main reactants are O_2, SO_2, SO_3, CO, CO_2, N_2, H_2O, Na_2SO_4. Deposition of metallic sulphates[8,9] (such as Na_2SO_4,$CaSO_4$) are found on the blades after service exposure and their effect[10] is known to be detrimental to the life of the blades. Different coatings[11,12,13] are applied to reduce environmental attack. During service the blades also go through thermal and mechanical cycling. In coated specimens, due to mismatch in the coefficients of thermal expansion between the coating and the substrate, a stress is developed at the interface. This stress varies during temperature cycling. Moreover, the coatings are ductile at high temperature and undergo more stress relaxation than the substrates. This might produce different strains in the coating and the substrate during thermo-mechanical cycling. The interfacial stresses might reduce the service life of the coated blades. Thermal and thermo-mechanical fatigue have been studied for ductile metals[14,15,16,17,18] and superalloys [19,20,21,22] Bizon, et al.[23] have done a comparative study of thermal

fatigue resistances of 26 nickel and cobalt-base superalloys.

At high operating temperatures interactions occur between the coating and the superalloy substrate. Due to diffusion the microstructure at the interface is different from the substrate and the coating. Both degradation and improvement in mechanical properties due to coating have been reported[24]. Smith[25] performed tensile tests, stress rupture tests and high cycle fatigue tests to examine the effect of low pressure plasma spray Co-29Cr-6Al-Y coating on IN 738 superalloy from room temperature to 870°C and found no significant effect on the coating and the coating process. Castillieo, et al.[26] studied the influence of chrome-aluminide coating on the creep and stress rupture properties of wrought Udimet 520 superalloy at 802°C. Their results showed that application of the chrome-aluminide coating caused a marked deterioration in rupture strength and ductility. Schweitzer, et al.[27] reported improvement in creep rupture life of IN 100 superalloy at 950°C due to low pressure plasma spray as well as electron beam physical vapor deposition (EBPVD) MCrAlY coating. Kang, et al.[28] observed that the application of low activity aluminide pack cementation treatment on directionally solidified Rene' 80 resulted in a dramatic reduction in rupture lives (83% at 760°C, 62% at 871°C and 36% at 982°C). The degradation was less severe for conventionally cast Rene' 80, but no reduction in rupture ductility was observed. Kolkman[29] studied the effect of Codep B coating (aluminum applied to the surface by low activity pack cementation) on the creep and fatigue properties of Rene' 80 at 900°C. The coating reduced the high cycle fatigue life by 62% and creep rupture life by 11%. Paskiet, et al.[30] performed fatigue tests on both uncoated and aluminide coated wrought

Udimet 700 superalloy over a range of temperature from 700 superalloy over a range of temperature from ambient to 927°C. The aluminide coating produced an enhancement of high cycle fatigue endurance limit up to 480°C, and above this temperature a slight reduction was observed. Schneider, et al.[31] reported a reduction in high cycle fatigue life in IN 738 LC and IN 939 nickel-base alloys at 850°C due to platinum-aluminide coating. Santhanam, et al.[32] observed improvements in thermal fatigue resistance (cycled between 27 and 944°C) in Udimet 710 superalloy due to plasma spray as well as EBPVD CoCrAlY coating. Rickerby, et al. [33] performed thermal shock tests on directionally solidified IN 738 LC superalloy by cycling between 20° and 1020°C and found that sputter ion-plated CoCrAlY coating improved the crack initiation time from ~150 - 200 cycles for uncoated specimens to 800 cycles for coated specimens. Strangman[34] studied thermo-mechanical fatigue of several nickel-base superalloys coated with NiCoCrAlY alloy. He observed that different phases between the temperature and load cycles required different numbers of cycles for crack initiation. Strang, et al.[35] has summarized data concerning the influence of coatings on mechanical properties. He concluded that, provided a suitable heat treatment was carried out after coating, no loss in creep rupture properties should be seen and that the coatings do not have a deleterious effect on low cycle fatigue life above the ductile-brittle transition temperature of the coating.

In the present program, thermal and thermo-mechanical fatigue of superalloy Rene' was studied. The effect of post heat-treated electron beam physical vapor deposition (EBPVD) CoCrAlY coating was investigated. To obtain

base line data, creep tests at elevated temperatures were performed for the coated and uncoated specimens. To understand the effect of the coating, detailed characterization of the microstructure at the interface between the coating and the substrate was done. In the following, the details of the work done is reported.

B. MATERIALS

Cylindrical pieces of cast blanks of Rene 80 were obtained from Arwood Corporation. They were machined to get specimens of gauge length 0.6 inch and gauge diameter 0.2 inch. The specimens were given the following heat treatment: first they were solutionized at 1205°C for 2 hours inside a cold wall vacuum furnace. The pressure in the furnace was about $5X10^{-6}$ torr throughout the heat treatment. They were rapidly cooled in vacuum (in less than 10 minutes) to 600°C and then cooled to room temperature. Then they were reheated to 1095°C and annealed for 4 hours. The specimens were vacuum cooled to room tempe ature and some of the specimens were taken out and sent for coating. The rest were annealed again in vaccum at 1050°C for 2 hours. The specimens were then cooled down rapidly (in less than 10 minutes) to 650°C and held at 650°C for 10 minutes. The specimens were reheated to 850°C and were aged at that temperature for 16 hours.

A CoCrAlY coating was applied by the Airco Temescal Corporation using the electron beam physical vapor deposition (EBPVD) technique. The surface of the specimens was prepared for coating by degreasing, grit blasting and vapor honing. The substrate temperature was 982°C and the pressure was about $5x10^{-4}$ torr throughout the coating process. The specimens were rotated by a gear arrangement for uniform coverage. The thickness of the

coating was about 80 μm. The composition of the coating and the substrate superalloy was given in Table I. The coated specimens were vacuum cooled for 5 minutes and then quenched in argon gas for 5 minutes. To close the pores during deposition the specimens were peened by glass beads to an Almen intensity of 15 N. To produce a diffusion bonding between the coating and the substrate, the specimens were heat treated at 1050°C for 2 hours in vacuum. The specimens were cooled in vacuum to ~ 550°C and then argon quenched. Finally, the coated specimens were aged in vacuum at 850°C for 16 hours. The coated and uncoated specimens underwent the same heat treatment.

C. THERMAL FATIGUE UNDER CREEP CONDITION

The initial part of the project involved a study of thermal cycling of coated and uncoated specimens under a constant load. A creep frame with an automatic leveller (made by Riehle) was used. Threaded grips with low heat loss was designed. The heating was done by a 5 KW induction unit (made by Lepel) running at 450 KHz. The induction coil surrounding the specimen was made from $^{3}/_{16}$ inch diameter copper tubing. The inner diameter of the coil was 1 inch and the length was ~ 3 inch. The geometry of the coil was designed to get uniform temperature (within ± 3°C) over the gauge length and to get a rapid heating (about 500°C per minute). The temperature of the specimen was monitored by thermocouples (K-type) welded to the shoulder of the specimen. Due to radio frequency (rf) pickup, the temperature measurement by thermocouple was not reliable. An emissivity independent infrared pyrometer (made by Vanzetti Corp.) was used to calibrate the

thermocouples.

The temperature cycling was controlled by a programmable controller (made by Leeds & Northup Co.,) having dual control outputs, one for heating and one for cooling. The fast cooling was achieved by blowing dry and cool air from a oil-free compressor connected with a refrigerator. A coil made of 0.5 inch diameter copper tube surrounded the specimen and the induction coil. A few holes were made on the inner side of the coil and the air blew through the holes on the specimen. The rate of air flow was controlled by a flow controller (made by Matheson Co.). The flow controller can take 0-5 volt input from the temperature controller and adjust the flow accordingly. The temperature was ramped up from 425°C to 925°C in 1 minute and held at 925°C for 0.5 minutes. It was then ramped down to 425°C in one minute and held at 425°C for 0.5 minutes. The temperature cycle was repeated. The specimen was kept under a constant load. The elongation was measured by an extensometer. Preliminary tests were performed to check the setup.

D. THERMO-MECHANICAL FATIGUE

In this part of the project, both the temperature and the strain were varied cyclically with different phases. In one case, the maximum temperature occured at the maximum strain and, in another case, the maximum temperature occured at the minimum strain. An MTS machine with a programmable controller (model #458.20) was used for strain cycling. The heating was done by an induction unit. A programmable temperature controller (made by Leeds & Northup Co.) performed the temperature cycling. A computer (made by Hewlett-Packard Co.) was connected to the MTS

machine and the temperature controller. The computer controlled the strain as well as the heating. The computer maintained a proper phase between the temperature and the strain. It also acquired data from the extensometer and the load cell. At present the software for control and data acquistition are being developed.

E. CREEP

Constant load creep tests were carried out for both coated and uncoated specimens in a creep frame attached with a furnace in air. The temperature was maintained at 1000°C and the stress was 138 MPa. The load for the coated specimens was calculated assuming uniform load bearing capacity of the coating and the substrate. The elongation was measured by a linear variable transformer.

Fig. 1 shows the strain vs. time curves for coated and uncoated specimens crept at 1000°C under a stress of 138 MPa. It is clear that the coated specimen elongates faster and breaks earlier. The rupture life is (71 ± 3) hours and (97 ± 5) hours for coated and uncoated specimens, respectively. The steady state creep strain rate for the coated and uncoated specimens are (8 ± 1) × 10^{-8}/s and (5 ± 0.5) × 10^{-8}/s, respectively. The rupture strain (calculated one hour before rupture) is about the same (~ 6.5%) in both cases.

F. MICROSTRUCTURE

The initial microstructure of the coated and the uncoated specimens after heat treatment was observed by a scanning electron microscope (SEM).

Some coated specimens were annealed at 1000°C for 100 hours to see how the diffusion zone grew. The specimens ruptured after the creep test were cut perpendicular and parallel to the load axis and observed in the SEM. Energy dispersive X-ray (EDX) spectroscopic analysis was also performed to find out the diffusion of different elements. To perform cross sectional transmission electron microscopy (TEM), thin slices were cut perpendicular to the axis of the cylindrical specimens. The slices were ground in emery paper and small discs containing coated area were punched out. The discs were then jet-polished and ion-milled to get suitable specimens with a thin area at the interface between the coating and the substrate.

The microstructures of the uncoated and the coated specimens before the creep test were the same. They consisted of cuboidal gamma prime precipitates[36] of ordered Ni3Al phase in Ni solid solution. The size of gamma prime precipitates was ~ 0.5 μm. The microstructure of the coating region consisted of the deposited coating and a diffusion zone growing inside the substrate. The coating contained CoAl precipitates. The diffusion zone of thickness about 3 μm grew inside the superalloy substrate due to the heat treatment after deposition of the coating. The diffusion zone contained NiCoAl precipitates. The precipitates were faceted and oriented in directions different from those in the coating. The diffusion zone did not contain any gamma prime precipitates. Kirkendall pores of ~ 0.5 μm size were observed at the interface between the coating and the diffusion zone. Some of the pores were seen to be faceted. Precipitates containing yttrium and other refractory metals were seen at the interface between the coating and the diffusion zone. The size of these precipitates were ~ 0.2 μm. Sigma

phase needles[37] were seen at the interface between the diffusion zone and the substrate.

Upon annealing in air at 1000°C for 100 hours the diffusion zone grew to ~ 10 μm inside the substrate. The thickness of the coating remained the same. The diffusion zone grew at the expense of the substrate. Kirkendall pores were also observed at the interface between the coating and the diffusion zone. Pores became ellipsoidal, but no change in pore size due to annealing at 1000°C for 100 hours was noticed. There was a precipipate-free region (about 1 μm in thickness) at the interface between the coating and the diffusion zone. This was due to depletion of Al which was taken up by (Ni,Co)Al precipitates.

The diffusion zone in the creep-ruptured specimen (life was 70 hours at 1000°C and 138 MPa) was ~ 8 μm. By comparing this size with that of the annealed specimen, and assuming that the diffusion distance varied as square root of time[38], one could conclude that the stress did not enhance the size of the diffusion zone. The orientations of (Ni,Co)Al precipitates did not depend on the stress. Kirkendall pores of the same size as in the case of the annealed specimens were observed. In addition, cavitation pores of ~ 5 μm size were seen at the interface of the coating and diffusion zones. Such cavitation was not observed at the coating-diffusion zone interface for annealed and as-coated specimens. So it is thought that under stress, some of the Kirkendall pores grew to cavity. The gamma prime precipitates were elongated perpendicular to the load axis. Similar elongation of gamma prime precipitates under stress were observed in other superalloys[5,39].

An aluminum oxide (Al_2O_3) layer of thickness of ~ 1 μm was formed on

the surface of all the coated specimens. A similar oxide layer was reported for the FeCrAlY coating[40]. There was a precipitate-free region beneath the aluminum oxide layer. In this region there was not enough Al to form CoAl precipitates.

To determine diffusion of different components, energy dispersive X-ray analysis was carried out in different regions of the coating, diffusion zone and the substrate. The presence of nickel was seen 2 μm below the surface. So Ni diffused out from the substrate almost to the top of the coating. The diffusion zone was richer in Co.

From the TEM work, it was seen that small Y_2O_3 precipitates[41] were present in the coating. It was also noticed that the CoAl precipitates in the diffusion zone grew as a single crystal while those in the deposited region were polycrystals.

During the heat treatment of the coated specimen, cobalt from the coating diffused into the superalloy substrate which contained Ni_3Al gamma prime precipitates. Addition of Co made Ni_3Al unstable[42,43]. (Ni,Co)Al precipitates were formed in the region where Co diffused. Extra Ni diffused out into the coating. The Co solid solution in the diffusion was h.c.p. in structure whereas the superalloy matrix was f.c.c. Due to the different structures there was a sharp boundary between the diffusion zone and the matrix. The thickness of the diffusion zone indicated the distance that Co diffused from the coating to the matrix. This distance was ~ 10 μm for specimens annealed at 1000°C in air for 100 hours. On the other hand, the EDX study showed that Ni diffused at least 70 μm into the coating. So the diffusion of Ni into the coating was faster than that of Co into the matrix.

That possibly led to the formation of Kirkendall pores at the interface between the coating and the diffusion zone. Such pores have been reported in Ni/Al[44] and Ni/Zr[45] systems. Nesbitt, et al.[46] found that after oxidation at 1150°C interdiffusion betweeen plasma sprayed Ni-16 at% Cr-25 at% Al-0.06 at% Zr coating and Ni-22 at% Cr substrate rapidly reduced the aluminum content of the coating and resulted in porosity at the coating-substrate interface. The pores have a deleterious effect on the mechanical properties of CoCrAlY coated Rene' 80 superalloy. The pores might act as nucleation sites for cracks and shorten the creep rupture life. As a matter of fact, creep cavitation were seen to be more prevalent at the interface between the coating and the diffusion zone.

Kang, et al.[28] have attributed reduction in creep rupture life of an aluminide coated Rene' 80 superalloy to cracking in the coating. CoCrAlY used in the present study has ductile-brittle transition temperature[13] at 650°C. The coating was ductile at the test temperature of 1000°C and no cracks were seen to initiate from the coating. Since the coating was deposited at a substrate temperature of 982°C and the test temperature was 1000°C, there was hardly any stress during the test at the interface due to mismatch in the thermal expansion coefficients of the coating and the substrate.

Sigma phase needles formed at the interface between the diffusion zone and the substrate are known to be brittle and might have had a deleterious effect[47] on the mechanical properties of the superalloy. Castillo, et al.[26] observed fracture paths associated with needle-like precipitates below the diffusion zone in chrome-aluminide coated Udimet 520 superalloy,

creep-tested at 802°C and 414 MPa. It is not clear from the present study whether they have any effect on the creep life of Rene' 80 at 1000°C. No cracks or cavities were seen near the sigma precipitates.

G. CONCLUSIONS

The experimental setup and preliminary testing of thermal cycling under creep conditions and thermo-mechanical fatigue have been performed. The steady creep test shows that the heat treated EBPVD CoCrAlY coating had a deleterious effect on the rupture life of Rene' 80. It reduced the rupture life by 30% at 1000°C and 138 MPa. A diffusion zone (~ 3 μm thick prior to the creep test), rich in CoAl precipitates, was observed at the interface between the coating and the substrate. This diffusion zone was due to the heat treatment given to the specimens after the deposition of the coating. The diffusion zone grew farther inside the substrate during the creep. Kirkendall pores of ~ 0.5 μm size were seen at the interface between the coating and the diffusion zone. The pores were formed due to faster diffusion of Ni into the coating than that of Co into the substrate. Experiments are in progress to determine the effect of microstructural modification on the thermal and thermo-mechanical fatigue properties of coated Rene' 80 superalloy.

REFERENCES

1. E.W. Ross, *Rene 80: A Cast Turbine Blade Alloy*, Metal Progress **99**, (1971) 93.

2. L.J. Fritz and W.P. Koster, *Tensile and Creep Rupture Properties of (16) Uncoated and (2) Coated Engineering Alloys at Elevated Temperatures*, NASA Tech. Report, NASCR-135138, NASA Lewis Research Center, Cleveland, OH, Jan. 1980.

3. D.M. Shah and D.N. Duhl, *The Effect of Orientation, Temperature and Gamma Prime Size on the Yield Strength of a Single Crystal Ni-Base Superalloy*, in Superalloy 1984, M.Gell, C.S. Kortovich, R.H. Bricknell, W.B. Kent and J.F. Radvitch, eds., Conference Proceedings, Met. Soc. of AIME, (1984) 105-114.

4. Y. Lindblom, *Creep and Structural Stability of High Temperature Materials*, in High Temperature Alloys for Gas Turbines, D. Coutsouradis, P. Felix, H. Fischmeister, L. Habraken, Y. Lindblom and M.O. Speidel, eds., Appl. Sci. Publishers Ltd., London, (1978) 285-316.

5. M.V. Nathal and L.M. Ebert, *Elevated Temperature Creep Rupture Behavior of the Single Crystal Nickel-Base Superalloy NASAIR 100*, Metall. Trans. A. **16A** (1985) 427.

6. Y. Han and M.C. Chaturvedi, *Steady State Creep Deformation of Superalloy Inconel 718*, Mater. Sci. Engr., **89** (1987) 25.

7. C.J. Spengler, *Characterization of Corrosion Attack of Superalloys in Combustion Turbines in the Temperature Range 600-760°C (1110-1400°F)*, in Superalloy 1980, J.K. Tien, S.T. Wlodek, H. Morrow III, M. Gell and G.E. Maurer, eds., Amer. Soc. Metals (1980) 395-404.

8. A.B. Hart, J.W. Laxton, C.G. Stevens and D. Tidy, *Deposition of Sodium Compounds Under Gas Turbine Conditions*, in High Temperature Alloys for Gas Turbines, D.Coutsouradis, P. Felix, H. Fischmeister, L. Habraken, Y. Lindblom, M.O. Speidel, eds., Appl. Sci. Publ. Ltd, London (1978) 81-107.

9. H. Gilder and R. Morbioli, *Sulphidation Behavior of Nickel- and Cobalt-Based Alloys*, ibid., 125-146.

10. D.A. Woodford and R.H. Bricknell, *Penetration and Embrittlement of Grain Boundaries by Sulphur and Chlorine--Preliminary Observations in Nickel and Nickel-Base Superalloys*, Scripta Met. **17** (1983) 1341.

11. P.G. Cappelli, *Coating Processes*, in High Temperature Alloys for Gas Turbines, D. Coutsouradis, P. Felix, H. Fischmeister, L. Habraken, Y. Lindblom, M.O. Speidel, eds., Appl. Sci. Publ. Ltd., London (1978) 177-189.

12. F.J. Pennisi and D.K. Gupta, *Improved Plasma-Sprayed Ni-Co-Cr-Al-Y and Co-Cr-Al-Y Coatings for Aircraft Gas Turbine Applications*, Thin Solid Films **84** (1981) 49.

13. K. Schneider and H. W. Grunling, *Mechanical Aspects of High Temperature Coatings*, ibid., **107** (1983) 395.

14. L.F. Coffin, Jr., *A Study of the Effects of Cyclic Thermal Stresses On a Ductile Metal*, Trans. ASME, **76** (1954) 931.

15. S. Taira, *Relationship Between Thermal Fatigue and Low Cycle Fatigue at Elevated Temperature*, in Fatigue at Elevated Temperatures, ASTM STP 520, A.E. Carden , A.J. McEvily and C.H. Wells, eds., Amer. Soc. for Testing & Mat. (1973) 80-99.

16. D. Eylon, D.G. Brandon and A. Rosen, *Creep Testing of Alpha Iron During Thermal Cycling*, ibid., 311-319.

17. E. Nes and P. Fartum, *Thermal Fatigue of Caster Shell Steels*, Scand. J. Metall. **12** (1983) 107.

18. H.J. Westwood, *High Temperature Fatigue of 304 Stainless Steel Under Isothermal and Thermal Cycling Conditions*, Fracture **2** (1977) 755.

19. G.P. Tilly, *Laboratory Simulation of Thermal Fatigue Experienced by Gas Turbine Blading*, in Thermal Stresses and Thermal Fatigue, D.J. Littler, ed., Butterworths Ltd., London (1970) 47.

20. A.E. Gemma, B.S. Langer and G.R. Leverant, *Thermomechanical Fatigue Crack Propagation in an Anisotropic (Directionally Solidified) Nickel-Base Superalloy*, in Thermal Fatigue of Materials and Components, ASTM STP **612**, D.A. Spera and D.F. Mowbray, eds., Amer. Soc. Testing & Mat. (1976) 199-213.

21. D.H. Boone and C.P. Sullivan, *Effect of Several Metallurgical Variables on Thermal Fatigue Behavior of Superalloys*, in Fatigue at Elevated Temperatures, ASTM STP **520**, A.E. Carden, A.J. McEvily and C.H. Wells, eds., Amer. Soc. Testing & Mat. (1973) 401-415.

22. D.F. Mowbray, D.A. Woodford and D.E. Brandt, *Thermal Fatigue Characterization of Cast Cobalt and Nickel-Base Superalloys*, ibid., 416-426.

23. P. T. Bizon and D.A. Spera, *Comparative Thermal Fatigue Resistances of Twenty-six Nickel- and Cobalt-Base Alloys*, NASA Tech. Report, NASA TN D-8071, NASA Lewis Research Center, Cleveland, OH, Oct. 1975.

24. L. Peichl and G. Johner, *High Temperature Behavior of Different Coatings in High-Performance Gas Turbines and in Laboratory Tests*, J. Vac. Sci. Technol., **A4** (1986) 2583.

25. R.W. Smith, *Mechanical Properties of a Low-Pressure-Plasma-Applied Co-Cr-Al-Y Coating*, Thin Solid Films **84** (1981) 59.

26. R. Castillo and K. P. Willett, *The Effect of Protective Coatings on High Temperature Properties of a Gamma-Prime-Strengthened Ni-Base Superalloy*, Metall. Trans. A. **15A** (1984) 229.

27. K.K. Schweitzer and G. Johner, *Summary Abstract: Performance Evaluation of Coatings for Jet Engine Turbine Blades by Sercicelike Tests*, J. Vac. Sci. Technol., **A3** (1985) 2525.

28. S.B. Kang, Y.G. Kim, H.M. Kim and N.S. Stoloff, *The Influence of a Coating Treatment and Directional Solidification on Creep Rupture Properties of a Nickel-Base Superalloy*, Mat. Sci. Eng., **83** (1986) 75.

29. H.J. Kolkman, *Creep, Fatigue and Their Interaction in Coated and Uncoated Rene 80*, ibid., **89** (1987) 81.

30. G.F. Paskiet, D.H. Boone and C.P. Sullivan, *Effect of Aluminide Coating on the High-Cycle Fatigue Behavior of a Nickel-Base High Temperature Alloy*, J. Inst. Metals, **100** (1972) 58.

31. K. Schneider, H. Von Arnim and H.W. Grunling, *Influence of Coatings and Hot Corrosion on the Fatigue Behavior of Nickel-Based Superalloys*, Thin Solid Films **84** (1981) 29.

32. A.T. Santhanam and C.G. Beck, *The Influence of Protective Coatings on Thermal Fatigue Resistance of Udimet 710*, ibid., **73** (1980) 387.

33. D.S. Rickerby and M.I. Wood, *Evaluation of Sputter Ion Plated CoCrAlY and NiCrAlTi Coatings for Gas Turbines*, J. Vac. Sci. Technol., **A4** (1986) 2557.

34. T.E. Strangman, *Fatigue Crack Initiation and Propagation in Electron Beam Vapor-Deposited Coatings for Gas Turbine Superalloys*, Thin Solid Films **45** (1977) 499.

35. A. Strang and E. Lang, *High Temperature Alloys for Gas Turbines 1982*, R. Brunetaud, D. Coutsouradis, T.B. Gibbons, Y. Lindblom, D.B. Meadowcroft and R. Stickler, eds., Reidel, Dordrecht, (1982) 469-506.

36. S.D. Antolovich and J.E. Campbell, *Fracture Properties of Superalloys in Superalloy Sourcebook*, Amer. Soc. Met. (1984) 112-169.

37. J.R. Mihalisin, C.G. Bieber and R.T. Grant, *Sigma-Its Occurence, Effect, and Control in Nickel-Base Superalloys*, Trans. Metall. Soc. AIME **242** (1968) 2399.

38. P.G. Shewmon, *Diffusion in Solids*, McGraw Hill, NY, NY (1963).

39. J.K. Tien and S.M. Copley, *The Effect of Uniaxial Stress on the Periodic Morphology of Coherent Gamma Prime Precipitates in Nickel-Base Superalloy Crystals*, Metall. Trans. **2** (1971) 215.

40. J.G. Smeggil and A.J. Shuskus, *The Oxidation Behavior of Some FeCrAlY, FeCrAl, and Yttrium Ion-Implanted FeCrAl Alloys Compared and Contrasted*, J.Vac. Sci. Technol. **A4** (1986) 2577.

41. J.R. Caol, G.H. Meier and F.S. Petit, *Transmission Electron Microscopy Characterization of the Microstructure of CoCrAlY Electron Beam Physical Vapor Deposition Coating on In 738*, ibid. **A4** (1986) 2915.

42. K.L.Luthra and M.R. Jackson, *Coating/Substrate Interactions at High Temperature*, G.E. Tech. Info. Series, 86CRD224, Corp. R&D, Schenectady, NY, Jan. 1987.

43. W.G. Moffatt, *Handbook of Binary Phase Diagrams*, Genium Publ. Corp., Schenectady, NY (1984).

44. M.M. P. Janssen and G.D. Rieck, *Reaction Diffusion and Kirkendall-Effect in the Nickel-Aluminum System*, Trans. Metall. Soc. AIME **239** (1967) 1372.

45. S.B. Newcomb and K.N. Tu, *Transmission Electron Microscopic Observation of Amorphous NiZr Alloy Formation by Solid-State Reaction*, Appl. Phys. Lett. **48** (1986) 1436.

46. J.A. Nesbitt and R.W. Heckel, *Modeling Degradation and Failure of Ni-Cr-Al Overlay Coatings*, Thin Solid Films **119** (1984) 281.

47. G.Chen, C. Yao, Z. Zhong and W. Yu, *The Effect of Sigma Phase on the Mechanical properties in Ni-Cr-Co Base Wrought Superalloys*, in Superalloys 1980, J.K. Tien S.T. Wlodek, H.G. Morrow III, M. Gell, G.E. Maurer, eds., Amer. Soc. Metals (1980) 355-364.

TABLE I

The Nominal Composition (Wt%) of the Coating and Substrate

	Ni	Co	Cr	Al	Ti	W	Mo	Y
Coating	x	66	23	10.5	x	x	x	0.25
Substrate	60.5	9.5	14	3	5	4	4	

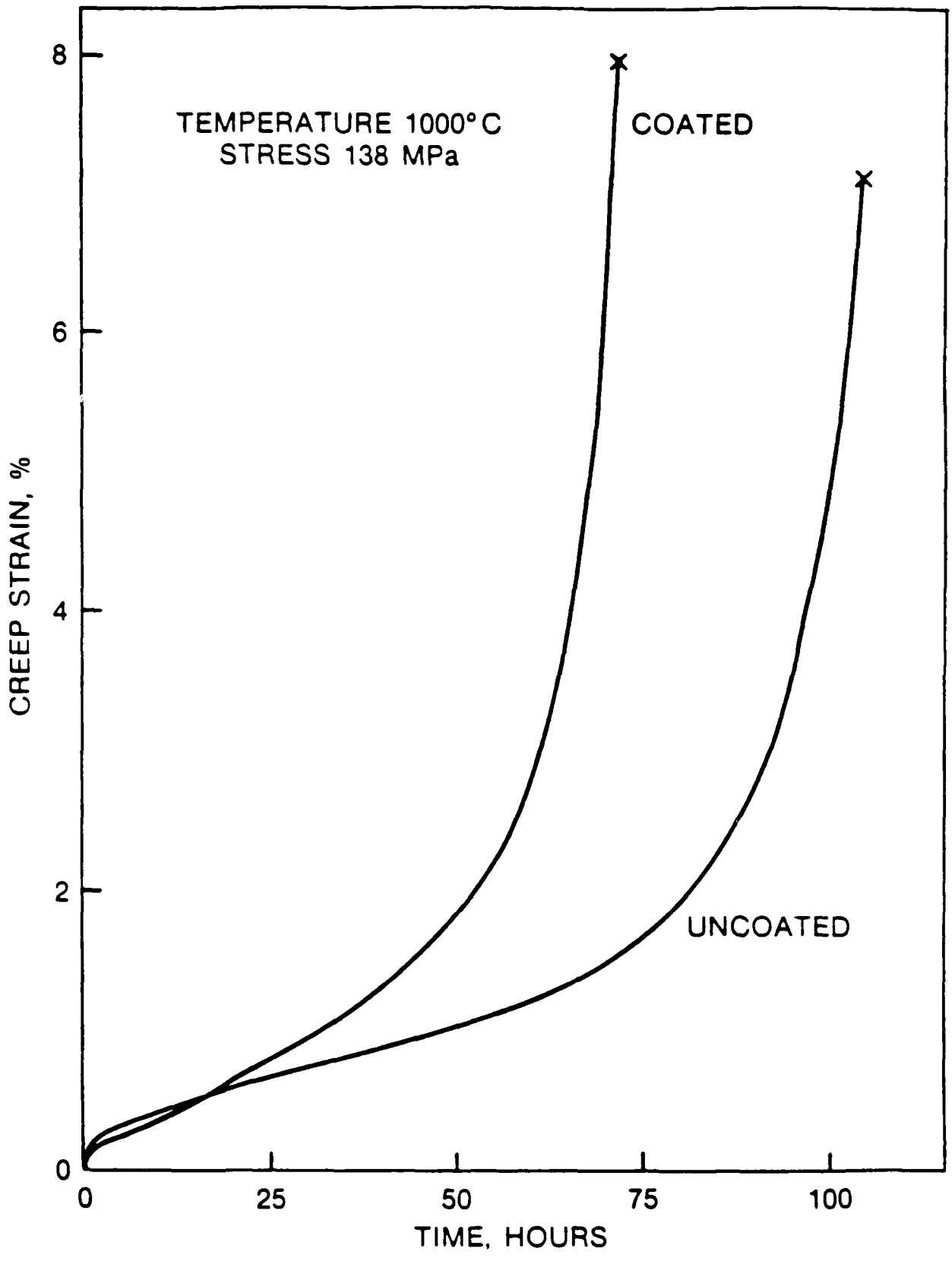

FIG. 1 Creep strain vs time for coated and uncoated representative samples.

END

10-87

DTIC